Article

Memory Effects in Compound-Specific D/H Analysis by Gas Chromatography/Pyrolysis/Isotope-Ratio Mass Spectrometry

Ying Wang, and Alex L. Sessions

More About This Article

Additional resources and features associated with this article are available within the HTML version:

- Supporting Information
- Access to high resolution figures
- Links to articles and content related to this article
- Copyright permission to reproduce figures and/or text from this article

View the Full Text HTML

Memory Effects in Compound-Specific D/H Analysis by Gas Chromatography/Pyrolysis/Isotope-Ratio Mass Spectrometry

Ying Wang* and Alex L. Sessions

Division of Geological and Planetary Sciences, California Institute of Technology, 1200 East California Boulevard, Pasadena, California 91125

Compound-specific analyses of lipid D/H ratios often encounter ranges of 300‰ or more, and experiments using D-enriched water to study fractionations often extend the range up to 1000‰. Here we show that for such large dynamic ranges in D/H ratio, isotopic "memory" between adjacent peaks can be significant. Memory effects have not been previously reported for GC/P/IRMS systems but can have a significant impact on many measurements, even those exploring only natural-abundance variations in D/H. To quantitatively evaluate these effects, we synthesized two series of organic standards with δD values varying from −230 to +800‰. We then analyzed chromatograms in which analyte δD values, retention times, or relative abundances were independently varied. For two sequential GC peaks, isotopic memory is measured to be typically 2−4% of the difference in δD values between the two. Roughly half of this effect can be attributed to unknown processes within the GC itself, and the other half to surface adsorption processes in the pyrolytic conversion of analytes to H_2. Isotopic memory increases with decreasing time separation between peaks, with decreasing analyte abundance, and with increasing age of pyrolysis reactors. A simple numerical model that simulates dynamic adsorption of H_2 on pyrolytic carbon can reproduce many aspects of the experimental data, suggesting that this is likely to be an important mechanism in isotopic memory. Several steps to mitigate memory effects in routine analyses are suggested.

Gas chromatography coupled to isotope-ratio mass spectrometry via a pyrolysis interface (GC/P/IRMS; also "thermal conversion", GC/TC/IRMS) provides a convenient analytical route to high-precision analysis of the hydrogen-isotopic composition (^{2}H/^{1}H, or D/H) of individual organic compounds.[1−5] Over the past decade, the methodology has been rapidly adopted in geochem-

istry,[6] environmental chemistry,[7] biochemistry,[8] and the petroleum and food/flavor industries.[9−11] In contrast to ^{13}C, whose natural abundance typically varies over ~50‰, the natural abundance of D in organic materials often ranges over 300‰ or more.[12] Moreover, studies using D-enriched tracers or water often extend this range to beyond 1000‰. This large range, coupled with the tendency of many materials to absorb and/or adsorb H_2, make compound-specific D/H analyses particularly susceptible to memory effects. We use the term "memory" here to indicate any situation in which the isotopic composition of a given chromatographic peak affects that of the following peak (or peaks), regardless of mechanism.

Isotopic memory effects are well-known during the conversion of H_2O to H_2 in vacuum lines using metal reductants, especially uranium.[13] Such effects are generally due to the absorption of hydrogen by hot metals and are typically overcome by repeated injections of each sample until a stable δD value is reached. Memory effects have also been reported for the pyrolysis of water over metal catalysts in continuous-flow analyses. Using an alumina pyrolysis reactor packed with C-coated Ni and operated at 1050 °C, Begley and Scrimgeour[3] showed that memory for successive injections of water amounted to ~1.6% of the difference in isotope ratios between the injections (~2600‰ for δD and ~150‰ for δ^{18}O). In a similar system using reduced Cr in the pyrolysis reactor, Morrison et al.[14] reported ~1% memory between successive injections of water differing in δD values by up to 1500‰. In an early GC/P/IRMS system with a pyrolysis reactor containing no metal catalyst and operated at 1200 °C, Scrimgeour et al.[15]

* To whom correspondence should be addressed. Department of Geological and Planetary Sciences, California Institute of Technology, Mail Code 100-23, 1200 East California Blvd., Pasadena, CA 91125. Phone: (626)395-6894. E-mail: ywjojo@gps.caltech.edu.

(1) Tobias, H. J.; Brenna, J. T. *Anal. Chem.* **1997**, *69*, 3148–3152.
(2) Burgoyne, T. W.; Hayes, J. M. *Anal. Chem.* **1998**, *70*, 5136–5141.
(3) Begley, I. S.; Scrimgeour, C. M. *Anal. Chem.* **1997**, *69*, 1530–1535.
(4) Hilkert, A. W.; Douthitt, C. B.; Schluter, H. J.; Brand, W. A. *Rapid Commun. Mass Spectrom.* **1999**, *13*, 1226–1230.
(5) Sessions, A. L. *J. Sep. Sci.* **2006**, *29*, 1946–1961.
(6) Xiong, Y. Q.; Geng, A. S.; Pan, C. C.; Liu, D. Y.; Peng, P. A. *Appl. Geochem.* **2005**, *20*, 455–464.
(7) Sauer, P. E.; Eglinton, T. I.; Hayes, J. M.; Schimmelmann, A.; Sessions, A. L. *Geochim. Cosmochim. Acta* **2001**, *65*, 213–222.
(8) Chikaraishi, Y.; Suzuki, Y.; Naraoka, H. *Phytochemistry* **2004**, *65*, 2293–2300.
(9) Hor, K.; Ruff, C.; Weckerle, B.; Konig, T.; Schreier, P. *J. Agric. Food Chem.* **2001**, *49*, 21–25.
(10) Hor, K.; Ruff, C.; Weckerle, B.; Konig, T.; Schreier, P. *Flavour Fragrance J.* **2001**, *16*, 344–348.
(11) Li, M. W.; Huang, Y. S.; Obermajer, M.; Jiang, C. Q.; Snowdon, L. R.; Fowler, M. G. *Org. Geochem.* **2001**, *32*, 1387–1399.
(12) Sessions, A. L.; Hayes, J. M. *Geochim. Cosmochim. Acta* **2005**, *69*, 593–597.
(13) Bigeleisen, J.; Perlman, M. L.; Prosser, H. C. *Anal. Chem.* **1952**, *24*, 1356–1357.
(14) Morrison, D. J.; Dodson, B.; Preston, T.; Weaver, L. T. *Rapid Commun. Mass Spectrom.* **2001**, *15*, 1279–1282.
(15) Scrimgeour, C. M.; Begley, I. S.; Thomason, M. L. *Rapid Commun. Mass Spectrom.* **1999**, *13*, 271–274.

tested for isotopic memory by alternately measuring *n*-alkane and fatty acid peaks that differed in δD values by 200‰. They concluded that no memory effects were observable above analytical precision ($\sim$5‰). A similar conclusion was reached by Sessions et al.[16] using a series of *n*-alkanes with δD values ranging from −256‰ to −42‰.

In both of these latter cases, memory effects of 1−2% would be very hard, if not impossible, to observe given typical analytical precision for δD values of 2−4‰. It thus remains uncertain if such effects exist in compound-specific D/H analyses. Although likely small, they are nevertheless potentially very significant. As a concrete example, microorganisms are commonly grown in waters with δD values ranging from near 0‰ up to 500‰ or higher.[17] The fractionation factor associated with lipid biosynthesis is then derived from the slope of a regression of lipid δD values on water δD values. A memory effect of 2% in the system used to analyze lipids from these samples would lead to a systematic bias of 20‰ in the estimated fractionation factor.

In the study described here, we synthesized multiple lipid standards with δD values varying by up to 1000‰, allowing us to demonstrate conclusively that isotopic memory effects do exist for GC/P/IRMS systems. These memory effects are typically 2−3% of the difference in δD values between successive peaks, can reach $\sim$5% for an aging pyrolysis reactor, and would result in significant errors for many types of natural samples if not accounted for. Mechanisms responsible for the memory effects are explored, and we present a model of hydrogen adsorption on graphite that can reproduce many aspects of the experimental observations. The results suggest several ways in which memory effects can be quantified and/or minimized in routine analytical operations.

METHODS

Materials. Tests utilized three types of materials for isotopic analyses: synthetic fatty acid esters, CH_4 (C.P. grade), and H_2 (ultrahigh purity). Fatty acid esters were prepared as follows. D-labeled ethyl palmitate (EP) and *n*-propyl palmitate (PP) were synthesized by reacting hexadecanoic acid ($2,2$-d_2, 98%; C/D/N ISOTOPES) with a mixture of the appropriate anhydrous alcohol and acetyl chloride (20:1) at 100 °C for 25 min. After cooling to room temperature, each ester was extracted in hexane, purified over silica gel, and the purity was checked by GC/MS. Each D-labeled ester was then mixed quantitatively with a stock solution of the same unlabeled ester (Sigma-Aldrich) in varying ratios to yield six standards each for EP and PP with δD values ranging between −230 and +800‰. Different combinations and amounts of the two esters were then further mixed and diluted to produce the sample solutions analyzed by GC/P/IRMS.

Values of δD for CH_4 and H_2 reference gases were determined using the GC/P/IRMS system by comparison to a series of *n*-alkanes with known δD values.[16] Importantly, the δD values of the *n*-alkanes, determined independently by offline combustion/reduction, and CH_4 and H_2 gases are similar, such that memory effects will have little influence on the measurements. The approximate δD values of synthetic esters were then measured
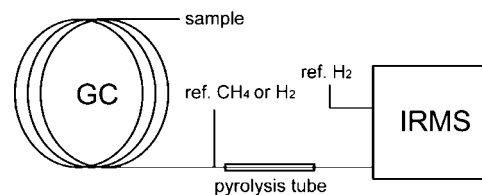

Figure 1. Simplified instrument schematic showing the pathways for delivery of sample, CH_4, and H_2 to the IRMS.

relative to the CH_4 reference gas. Because they differ considerably in D/H ratio they are, of course, subject to the same memory effects that we are attempting to measure. There are no certified isotopic standards (organic, water, or otherwise) with δD values above 0‰, so our measurements of δD values for these D-enriched materials are highly precise but of unknown accuracy. To avoid this complication, all of our tests focused on apparent changes in measured δD values, independent of the "true" δD values for these standards.

Isotopic Analyses. Compound-specific D/H analyses were performed on a ThermoElectron Trace GC coupled to a Delta-^{plus}XP IRMS via a ThermoElectron thermal conversion interface, consisting of an Al_2O_3 pyrolysis tube (0.8 mm i.d. and 305 mm long) operated at 1440 °C and an open split. No Nafion drier was employed. The GC was equipped with a programmable temperature vaporization (PTV) injector operated at a split ratio of 1:10, with a 2.0 mm i.d. metal liner (Siltek deactivated) packed with $\sim$7 cm of silanized glass wool. An EC-1 analytical column (30 m long, 0.32 mm i.d., 1.0 μm stationary phase; Alltech Associates) was used with helium carrier gas at 1.4 mL/min. The GC oven temperature was 100 °C for 3 min, 20 °C/min to 180 °C, then 5 °C/min to 280 °C for all analyses. All connections within the GC and pyrolysis interface were made with methyl-deactivated fused silica tubing (SGE) and stainless steel fittings (Valco Instruments)

To provide peaks of an organic reference gas in sample chromatograms, CH_4 ($\delta D = -148$‰) or H_2 ($\delta D = -171$‰) reference gas was diluted into a stream of helium which then filled a 20 μL sample loop on a six-port sampling valve (Valco Instruments). This valve was used to deliver discrete peaks of the reference gas into the GC system at a point immediately downstream from the analytical column (Figure 1). Peak heights were varied by changing dilution of the sample gas. Peak widths are approximately the same as for GC analyte peaks. This approach allowed us to insert peaks of known size and isotopic composition at any point in the chromatogram, such that they are still subject to pyrolytic conversion. In addition, another H_2 reference gas ($\delta D = -150$‰) was diluted into a second helium gas stream and flowed directly into the IRMS ion source (Figure 1) using the stock ThermoFinnigan GC II/III interface. These peaks, which are also variable in size and timing, do not experience any of the potential memory effects associated with the GC and pyrolysis systems.

Mass-2 and -3 signals were processed using ISODAT NT 2.5 software (ThermoElectron), and data are reported as δD values relative to Vienna standard mean ocean water (VSMOW) in permil units. To correct for H_3^+ interference,[16,18] the H_3^+ factor was determined daily by measuring the mass 3/2 signal ratio of 10

(16) Sessions, A. L.; Burgoyne, T. W.; Hayes, J. M. *Anal. Chem.* **2001**, *73*, 192–199.
(17) Zhang, Z.; Sachs, J. P. *Org. Geochem.* **2007**, *38*, 582–608.

(18) Sessions, A. L.; Burgoyne, T. W.; Hayes, J. M. *Anal. Chem.* **2001**, *73*, 200–207.

injections of H_2 reference gas at varying peak height. The value of the H_3^+ factor was very stable at 2.9–3.2 ppm/mV, and all H_3^+ corrections were performed via the ISODAT software. To minimize variations in δD values due to changing background conditions between GC runs, the following protocol was used for all sample analyses. Each chromatogram consisted of four peaks of CH_4 reference gas, followed at a 100 s interval by the analytes to be measured. A second series of two CH_4 peaks followed the analytes. All peak sizes were kept constant at 16 ± 2 V s for CH_4 and 20 ± 2 V s for the esters (expressed as the integrated mass-2 peak area), except where noted below. The final CH_4 peak from the first set, before the esters, was used as the calibration peak for all experiments with an assigned value of −148‰.

Raman Spectroscopy. Thin layers of carbonaceous material were obtained from the inner wall of used pyrolysis tubes. Raman spectroscopy of this material was performed using a Renishaw RM1000 micro-Raman spectrometer, operating with a 514.5 nm Ar ion laser with spectral resolution of 1 cm^{-1}. An optical microscope was used to focus the excitation laser beam on a sample area of 20 μm in diameter. The acquisition time was 30 s, and 10 spectra were recorded for each sample.

Numerical Model. To quantitatively explore the effect of hydrogen adsorption in the pyrolysis reactor on memory effects, we developed a simple numerical model to simulate the flow of analyte peaks through a pyrolysis reactor. The key feature of this model is explicit treatment of hydrogen adsorption on graphite lining the reactor. Gas residence times within a hot pyrolysis reactor are much shorter than typical analyte peak widths, and the thermal decomposition of analytes to H_2 is in turn faster than gas residence time. The input flow to the reactor was therefore simulated as a sequence of discrete H_2 gas parcels, with no concentration or isotopic gradient within the reactor. The concentrations and D/H ratios of gas parcels in the input stream are varied sequentially to simulate chromatographic peaks. H_2 in the input stream is allowed to interact with adsorption sites evenly coated on the inner wall of the pyrolysis reactor during its transit. The concentration and D/H ratio of H_2 gas exiting the reactor are calculated and recorded as the output "signal" (see the Supporting Information for details of the model and algorithm). Model output is then used to calculate δD values as described by Ricci et al.[19] and Sessions.[5]

Parameters required by the model include (i) the number of adsorption sites lining the reactor tube, which is estimated as the product of available carbonaceous material (typically 0.8–1.0 mg) in used pyrolysis tubes and the concentration of strong (~20 appm) or weak (~200 appm) adsorption sites in pyrolytic carbon;[20] (ii) desorption rate constant for hydrogen adsorbed to these sites, estimated to be ~1.1 s^{-1} based on the relevant C–H bond dissociation energy (see Theory and Model Section); (iii) the average concentration of H_2 in a typical chromatographic peak, which is estimated as ~890 Pa using typical carrier gas flow rate, dimensions and temperature of the reactor tube, peak shape (assumed to be Gaussian with $\sigma = 5$ s) and the amount of injected analyte (50 nmol H_2); and (iv) the concentration and D/H ratio

(19) Ricci, M. P.; Merritt, D. A.; Freeman, K. H.; Hayes, J. M. *Org. Geochem.* **1994**, *21*, 561–571.
(20) Kanashenko, S. L.; Gorodetsky, A. E.; Chernikov, V. N.; Markin, A. V.; Zakharov, A. P.; Doyle, B. L.; Wampler, W. R. *J. Nucl. Mater.* **1996**, *237*, 1207–1212.

Table 1. Summary of Experimental Conditions

expt	n^a	peak 1		peak 2		Δt (s)^c	$A_2/A_1{}^d$
		ID^b	δD (‰)	ID^b	δD (‰)		
A	6	EP	−225 to +730	PP	−204	100	1.0
B	6	EP	−225 to +730	CH_4	−148	100	0.8
C^e	5	EP	−225 to +730	CH_4	−148	100	0.8
D	6	EP	−225 to +730	H_2	−171	100	0.8
E	8	EP	639	CH_4	−148	100–800	0.8
F	5	CH_4	−148	EP	639	100–500	1.2
G	6	CH_4	−148	EP	672	100	0.22–2.23
H	5	EP	−238 to 526	PP	179	100	0.67
I	6	EP	−238 to 742	PP	179	100	1.24
J	6	EP	−238 to 742	PP	179	100	1.90

^{a} Number of different chromatograms analyzed in the experiment. ^{b} EP = ethyl palmitate; PP = *n*-propyl palmitate. ^{c} Time separation between peaks 1 and 2. ^{d} Abundance ratio for peaks 1 and 2, defined by mass-2 peak area. ^{e} H_2 peak added midway between peaks 1 and 2.

of background hydrogen in the carrier gas. This last quantity is impossible to measure directly because of isobaric interferences from $^4He^{2+}$ and $^3He^+$. On the basis of experimental data described below, we estimated the hydrogen background to be ~20 pA (20 mV measured signal) with a δD value between −200 and −300‰. An average δD value of −250‰ is adopted for background hydrogen in the model.

EXPERIMENTAL SECTION

Memory effects were investigated experimentally by analyzing multiple combinations of fatty acid esters, CH_4 reference gas, and/or H_2 reference gas. Each analysis (i.e., a single GC/P/IRMS chromatogram containing multiple peaks) contained the same analytes, typically two esters plus multiple reference gas peaks. The abundance and δD values of esters in any given chromatogram were manipulated by altering the composition of the solution injected into the GC. The timing of CH_4 and H_2 reference gas peaks relative to these esters was manipulated in each chromatogram directly via the ISODAT software. Multiple chromatograms were then analyzed in series that were arranged such that individual chromatograms differed systematically in either (i) δD values, (ii) retention times, or (iii) relative abundances. A single "experiment" (as defined in Table 1) consisted of one such series of multiple chromatograms.

Because accurate δD values for the D-enriched esters could not be readily determined, we instead looked for correlations between the measured δD values of peaks and the systematic differences between chromatograms. Those correlations allow us to quantitatively document the existence of memory effects, their functional dependence on different operating parameters, and their likely source(s) within the analytical system. Experimental results are summarized first, followed by a discussion of probable mechanisms leading to the observed effects.

Variation in D/H Ratios. Two initial experiments were conducted to look for memory effects, each consisting of six chromatograms. In the first experiment (A in Table 1), each chromatogram contained ethyl palmitate (EP) and propyl palmitate (PP) at equal concentrations and constant time separation. The δD values of peak 1 (EP) varied between chromatograms, while that of peak 2 (PP) was held constant. Measured δD values for peak 2 were found to vary systematically with those of peak 1,
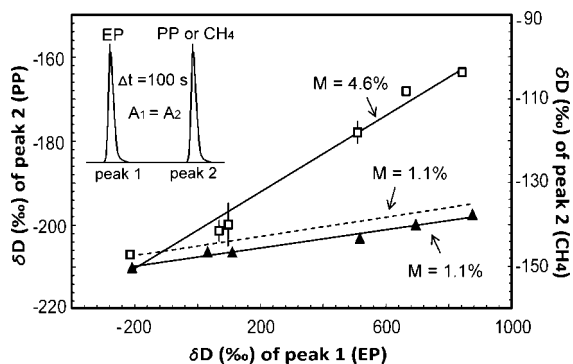
Figure 2. Demonstration of isotopic memory between two peaks of differing δD values. Specific test conditions are illustrated by the inset chromatograph and are summarized in Table 1. □, expt A, (EP + PP); ▲, expt B, (EP + CH₄). Standard deviations from 2 to 3 replicates are shown on measured data points and are usually smaller than the symbols. M is the slope of the correlation and indicates the size of the observed memory effect. The dashed line is the modeled memory effect using conditions of expt B (shifted upward from expt B data for clarity), as discussed in the Theory and Model Section.

Table 2. Summary of Memory Effects Measured between Adjacent Pairs of Peaks with Differing δD Values

EP + PP tests		EP + CH₄ tests		EP + H₂ test		
M (%)	$\sigma_M{}^a$	M (%)	$\sigma_M{}^a$	M (%)	$\sigma_M{}^a$	tube age^b
3.1	0.1	1.2	0.1	N/A		10−50
N/A		0.80	0.05	2.1	0.1	40−70
1.6	0.2	1.1	0.1	N/A		20−90
4.7	0.2	1.2	0.1	N/A		150−220
4.6	0.7	3.7	0.2	N/A		250−340

^{a} Standard error of the regression slope at 95% confidence level.
^{b} Cumulative number of analyses using that reactor tube.

with a correlation slope of 0.046 and R^2 value of 0.99 (Figure 2). In the second experiment (B), peak 2 consisted of CH₄ reference gas instead of PP. Again, the measured δD values for peak 2 varied systematically with those for peak 1, although this time with a lower correlation slope (0.011; Figure 2). Both results clearly demonstrate the existence of an isotopic memory effect.

In these experiments, the slope of the correlation line is a quantitative measure of how much the isotopic composition of one peak affects that of the next. It thus serves as a convenient metric for the size of the memory effect, which we denote as M ($= \Delta\delta_2/\Delta\delta_1$). It is also conceptually equivalent to the fraction of H₂ from one peak that is carried over to the next peak, though that need not be the physical mechanism by which memory exerts its influence. The value of M depends strongly on the specific test conditions used to determine it, including choice of compounds, time separation, peak size, and potentially instrument conditions. When these parameters are held constant, such as by using the EP + PP or EP + CH₄ test series, the values of M could be used for quantitative comparison of memory effects over time or between analytical systems.

The value of M was found to be systematically higher in experiments employing EP + PP compared to those using EP + CH₄ (Table 2). The only substantive difference between the experiments was that CH₄ peaks did not go through the GC

injector or column, while PP peaks did. We thus infer that part of the memory effect is localized within one or both of those components. The magnitude of M attributable to the GC is estimated to be 0.5−3.5%. To further pinpoint other sources of memory, a third experiment (C) introduced peaks of H₂ reference gas midway between peaks 1 and 2, with all other conditions identical to expt B. The measured values of M were identical both with and without H₂ peaks (data not shown), indicating that these H₂ peaks did not contribute to isotopic memory. We conclude that the IRMS itself does not cause any detectable memory, consistent with previous investigations using dual-inlet techniques.[13] The remaining memory effect (1.1−3.7%) must then be attributed to the pyrolysis reactor itself. Indeed, the value of M is roughly correlated with the age of the pyrolysis reactor tubes (Table 2), consistent with the expectation that memory increases as pyrolytic carbon accumulates in the reactor tube. In a fourth experiment (D), peak 2 consisted of H₂ reference gas ($\delta D = -171‰$) inserted using the same peak generator as for CH₄ (Figure 1). In this experiment, the value of M was measured to be about 2.5 times larger than that measured in the EP + CH₄ test during the same period of the reactor (Table 2). This result suggests that some sources or sites of isotopic memory are accessible to H₂ but not to CH₄ (see Theory and Model Section).

Variation in Time Separation. The dependence of memory effects on the time separation (Δt) between two peaks was investigated in two further experiments. In expt E, each chromatogram contained D-enriched EP (peak 1; 639‰) followed by CH₄ (peak 2; −148‰) with Δt varying between 100−800 s. As Δt increased, the measured δD value of peak 2 decreased systematically toward the "true" value (Figure 3a). The data are consistent with a simple decrease in memory as the time separation between peaks increases. However, as a further test the order of these two peaks was reversed (expt F), with CH₄ (peak 1) appearing 100−500 s before EP (peak 2). Surprisingly, as Δt increased the measured δD value of peak 2 decreased, just as before (Figure 3b). A plausible explanation is that there is a second component of isotopic memory, namely, background hydrogen in the helium carrier gas. The source of this background could be any species that yields H₂ on pyrolysis, including H₂O. As Δt between peaks increases, the isotopic composition of background hydrogen should exert a progressively greater influence on whatever pool of stored H is causing the memory effects. Thus if background hydrogen is more D-depleted than peak 1, then the δD value of peak 2 will appear to decrease with increasing Δt, consistent with data of both experiments E and F. This idea is explored further in the Theory and Model Section.

Variation in Relative Abundance. The effect of analyte abundance on memory was investigated in expt G. Each chromatogram in the series contained CH₄ reference gas (peak 1; −148‰) followed by D-enriched EP (peak 2; 672‰), with EP present in gradually increasing amounts. In Figure 4a, measured δD values for peak 2 are plotted against its abundance relative to peak 1, expressed as the ratio of peak areas (A_2/A_1). As the abundance ratio increases from 0.22 to 2.23, measured δD values of peak 2 systematically increased from 583‰ to 712‰ and tended toward a constant value at still higher ratios. These results are consistent with a decrease in memory with increasing analyte abundance.
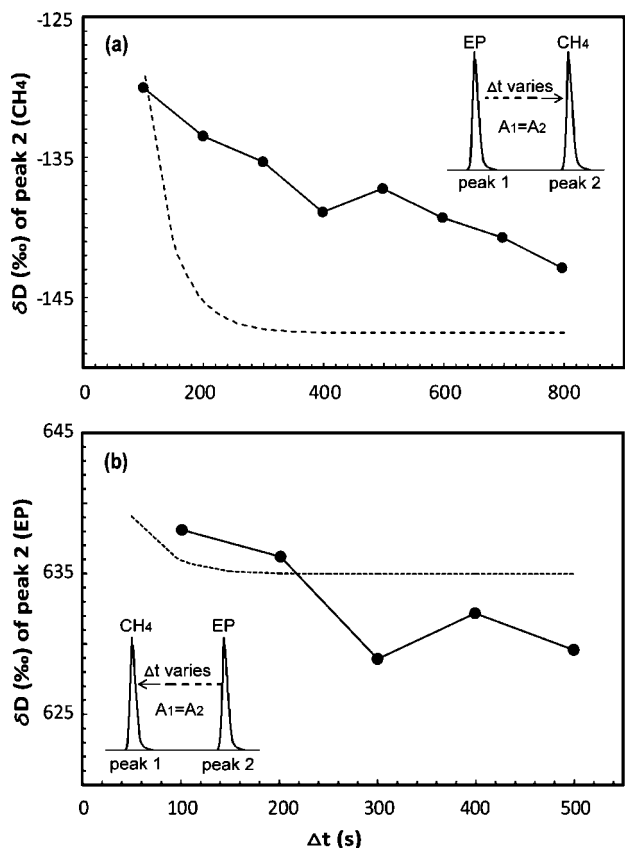
Figure 3. Dependence of isotopic memory on the time separation between adjacent peaks: (a) expt E (EP + CH$_4$); (b) expt F (CH$_4$ + EP). The symbols are experimental data, and the dashed lines are the model results.

Three further experiments (H−J) employed EP (peak 1) with variable δD values, followed by D-enriched PP (peak 2) with the δD value fixed at 179‰. These experiments are identical to expt A, except that the A_2/A_1 ratios were 0.67, 1.24, and 1.90 in experiments H, I, and J, respectively (Table 1). Values of M were calculated as before. As the A_2/A_1 ratio tripled, the value of M decreased from 3.4% to 2.1% (Figure 4b), consistent with expt G. However, if memory effects manifested in peak 2 were solely due to hydrogen contained in peak 1, there should be no observable memory when the δD values of the two peaks are equal. Thus the three curves in Figure 4b would be expected to intersect at a δD value near 179‰. This is clearly not the case, and the participation of background hydrogen in the memory phenomenon offers a potential explanation. If background hydrogen is always D-depleted relative to peak 1, its presence will tend to shift the measured δD values for peak 2 downward. This effect will be more pronounced when peak 2 is smaller, leading to the position of the three curves in Figure 4b.

THEORY AND MODEL SECTION

Physical Basis for Memory Effects. Numerous physical and chemical mechanisms could lead to isotopic memory effects in GC/P/IRMS systems. The most obvious candidates are those that result in physical transfer of hydrogen from one peak to the next. Alternatively, certain system conditions might systematically change as a result of interactions with organic analytes, such that the conversion or analysis of a given peak is subtly altered by the
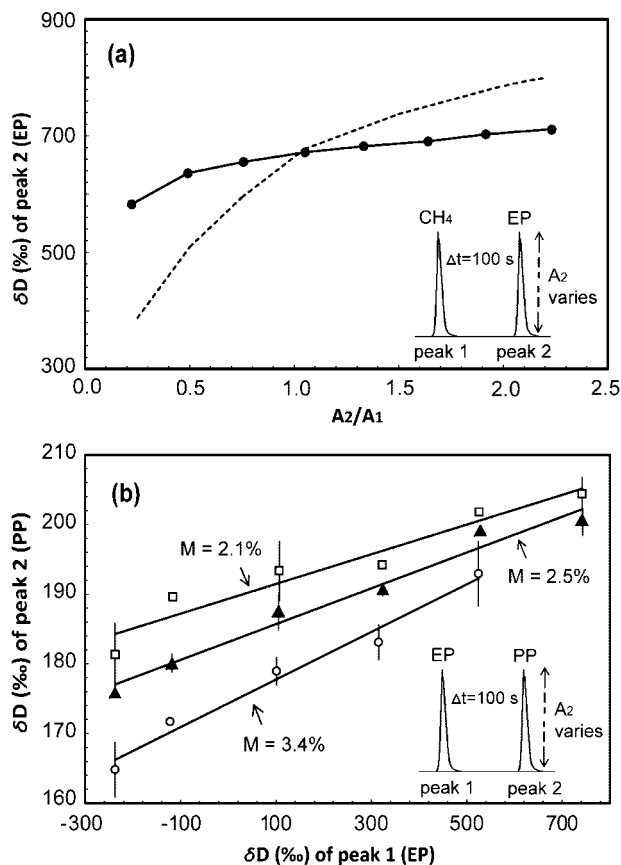
Figure 4. Dependence of isotopic memory on analyte abundance. (a) Changing abundance of peak 2 with constant δD value (expt G). (b) Changing δD values of peak 1 for three different A_2/A_1 ratios. ○, expt H ($A_2/A_1 = 0.67$); ▲, expt I ($A_2/A_1 = 1.24$); □, expt J ($A_2/A_1 = 1.90$). Error bars are standard deviations from duplicate analyses. The symbols are experimental data, and the dashed line is the model result.

presence of those preceding it. As a concrete example, pyrolysis of an organic analyte will deposit fresh carbonaceous material within the pyrolysis tube and might alter its reactivity for some short time span. While such phenomena might lead to the observed changes in δD with Δt or A_2/A_1, they cannot plausibly produce the systematic changes observed between peaks differing only in δD values. Changes in δD of several hundred permil represent changes in absolute D content of only a few parts per million. We therefore believe that the observed memory effects are caused primarily by molecule−surface interactions that lead to hydrogen storage and thus hydrogen transfer, specifically (i) adsorption of hydrogen on surfaces, (ii) absorption of hydrogen into solid materials such as tubing or fittings, and/or (iii) direct isotopic exchange between gas-phase molecules and hydrogen that is covalently bound in solid materials.

Mechanism 3 (direct isotopic exchange) seems most likely to cause memory effects that are localized within the GC system, which represent roughly half of all those observed here. When a highly D-labeled (~98% D) analyte is injected into the GC, the D/H ratios of all subsequent peaks, even in subsequent chromatograms following extensive bakeout, are substantially increased (A. Sessions, unpublished data). This effect can be reversed only by replacing the analytical column. Surface-bound methyl groups are of course abundant in the stationary phase of the GC column employed here (100% dimethylpolysiloxane) and

in the capillaries made of methyl-deactivated fused silica. However, isotopic exchange of C-bound H in gas-phase molecules at temperatures below 300 °C has not to our knowledge been previously reported. Very slow isotopic exchange has been reported in condensed (liquid or adsorbed) phases but only under activation by strong catalysts.[21,22] Direct H exchange could occur in the injector but would affect all analytes equally because they are not yet separated. This could not produce the memory effects observed here, in which the δD value of one peak depends on that of the previous one. We are thus unable to suggest a specific mechanism to explain the phenomenon. Nevertheless, the observation suggests that there is indeed exchange within the GC column via some unknown mechanism. A systematic comparison of memory associated with stationary phases and analytes of varying chemistry would help to elucidate the mechanism.

In contrast, mechanisms 1 and 2 (adsorption and absorption) are more likely to cause memory effects that are localized in the pyrolysis reactor and associated fittings and tubing. This reactor consists of a narrow-bore, 99.8% alumina tube heated to 1440 °C (measured near its midpoint), connected to fused-silica capillary tubing at both ends, through which chromatographic effluents continuously flow. Connections in this system are made with stainless-steel fittings, which can be considered as a potential source for memory. The solubility of hydrogen in Fe has been measured at ~0.03 nmol of H_2/g of metal at 400 K in equilibrium with 101 kPa H_2 (ref 23). The solubility decreases exponentially with temperature and pressure. At typical GC/P/IRMS operating conditions ($10-10^3$ Pa H_2 and <50 °C), hydrogen absorption in metal fittings is therefore negligible. Many oxides, including Al_2O_3, SiO_2, and Fe_2O_3, can acquire surface hydroxyl groups from ambient water[24] which might then undergo hydrogen exchange with gas-phase H_2. While we have no specific data regarding H_2-OH exchange rates, the equilibration of H_2 with H_2O occurs very slowly at room temperature without Pt catalysts and takes several days even with them.[25] Surface OH groups within the hot alumina pyrolysis tube itself might also be considered. However, these surface hydroxyl groups tend to desorb as water according to the equilibrium $Al_2O_3 + 3H_2O \leftrightarrow 2Al(OH)_3$ at temperatures above 1000 °C (refs 26 and 27), so the size of this exchangeable reservoir is likely small.

Dissection of used alumina reactor tubes reveals that pyrolysis deposits carbonaceous material over a 5–8 cm length near the upstream end of the tube, while the rest of the tube remains bare. He-atom scattering experiments,[27] in which alumina surfaces were exposed to molecular or atomic hydrogen both at room temperature and at 1200 K, show that there is virtually no hydrogen retained on bare surfaces. At room temperature, H_2 molecular adsorption on alumina surfaces is negligible[28] while dissociative

adsorption (i.e., as H atoms) is limited by the large bond dissociation energy for H_2 (ref 27). At high temperatures, it is proposed that H atoms adsorb onto the surface as OH species but then quickly react with other impinging H atoms to form water molecules which desorb. This process can lead to hydrogen etching of the alumina surface and might contribute to the observed increase in porosity of pyrolysis tubes as they age.[2,5] While we are not aware of similar experimental data for hydrogen adsorption on silica surfaces, that process seems equally unlikely to cause memory effects for all the same reasons.

Many carbonaceous materials have high gas-storage capacity (i.e., absorption) due to their relatively high porosity. Assuming a typical pore volume of ~0.5 mL/g for activated carbon[28] and typical operating conditions for GC/P/IRMS of 1440 °C, 1 mg of pyrolytic carbon, and $P_{H_2} = 900$ Pa, hydrogen storage within the entire pyrolysis reactor would be ~0.06 nmol of H. This represents only about 0.1% of the H_2 in a typical analyte peak and so is unlikely to be a major source of the observed memory effects. In contrast, carbonaceous materials also have a high affinity for surface adsorption of H_2 to an extent that could quantitatively explain the memory effects we observe. We therefore focus specifically on hydrogen adsorption onto graphite surfaces as a model for the processes responsible for isotopic memory in the pyrolysis reactor.

Hydrogen−Graphite Interactions. Hydrogen can adsorb onto graphite surfaces in a variety of ways. On the surface of the aromatic plane, adsorption occurs both through molecular or dissociative adsorption. Adsorption enthalpies (ΔE) for these two mechanisms are 0.04 eV (ref 29) and 0.7 eV (refs 30 and 31). Carbon atoms at the truncated edges of the aromatic plane are known to have dangling bonds that can form very strong C−H bonds ($\Delta E = 4.45$ eV) (refs 20 and 32), while nearby dangling bonds can interact with one another to form a "relaxed" structure which lowers the bond energy by ~1 eV. For carbon atoms at the edge of interstitial loops and in-plane defects, this relaxation is prevented by the surrounding carbon lattice. ΔE for hydrogen adsorption at relaxed and unrelaxed edge carbon atoms can thus be estimated to be 2.4 eV (weak sites) and 4.4 eV (strong sites), respectively.[20]

Figure 5 shows the Raman spectrum of carbonaceous material recovered from a used pyrolysis tube. The band of highest frequency (1580 cm^{-1}) is the G band corresponding to stretching vibrations in aromatic layers. The 1350 cm^{-1} band (D1 band) is attributed to in-plane defects and heteroatoms, and a weak wide band at 1500 cm^{-1} (D3 band) is attributed to defects outside the plane of aromatic layers (e.g., tetrahedral units).[33] They indicate that the pyrolytic carbonaceous material is composed of poorly organized aromatic sheets and tetrahedral fragments that expose abundant edges and in-plane defects, potential sites for hydrogen adsorption.

To evaluate the possibility that hydrogen adsorption produces isotopic memory effects, we first calculate the equilibrium surface coverage (θ, the ratio of occupied to total adsorption sites) as a

(21) Sessions, A. L.; Sylva, S. P.; Summons, R. E.; Hayes, J. M. *Geochim. Cosmochim. Acta* **2004**, *68*, 1545–1559.
(22) Larcher, A. V.; Alexander, R.; Rowland, S. J.; Kagi, R. I. *Org. Geochem.* **1986**, *10*, 1015–1021.
(23) Sieverts, A. *Z. Phys. Chem., Stoechim. Verwandtschaftsl.* **1911**, *77*, 591–613.
(24) Wang, X. G.; Chaka, A.; Scheffler, M. *Phys. Rev. Lett.* **2000**, *84*, 3650–3653.
(25) Coplen, T. B.; Wildman, J. D.; Chen, J. *Anal. Chem.* **1991**, *63*, 910–912.
(26) Ahn, J.; Rabalais, J. W. *Surf. Sci.* **1997**, *388*, 121–131.
(27) Woll, C. *J. Phys.: Condens. Matter* **2004**, *16*, S2981–S2994.
(28) Nijkamp, M. G.; Raaymakers, J. E. M. J.; van Dillen, A. J.; de Jong, K. P. *Appl. Phys., A* **2001**, *72*, 619–623.
(29) Ghio, E.; Mattera, L.; Salvo, C.; Tommasini, F.; Valbusa, U. *J. Chem. Phys.* **1980**, *73*, 556–561.
(30) Zecho, T.; Guttler, A.; Sha, X. W.; Jackson, B.; Kuppers, J. *J. Chem. Phys.* **2002**, *117*, 8486–8492.
(31) Sha, X. W.; Jackson, B. *Surf. Sci.* **2002**, *496*, 318–330.
(32) Atsumi, H.; Iseki, M. *J. Nucl. Mater.* **2000**, *283*, 1053–1056.
(33) Beyssac, O. *Spectrochim. Acta, Part A* **2003**, *59*, 2267–2276.
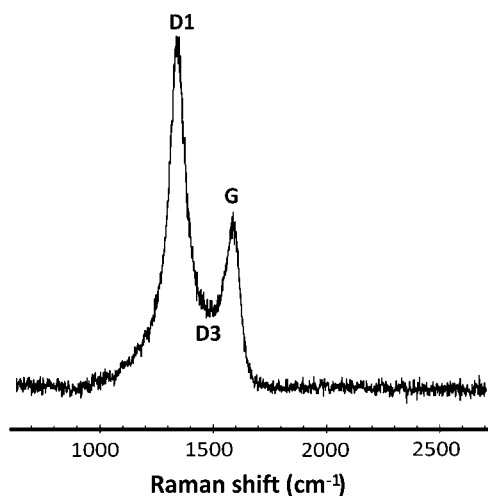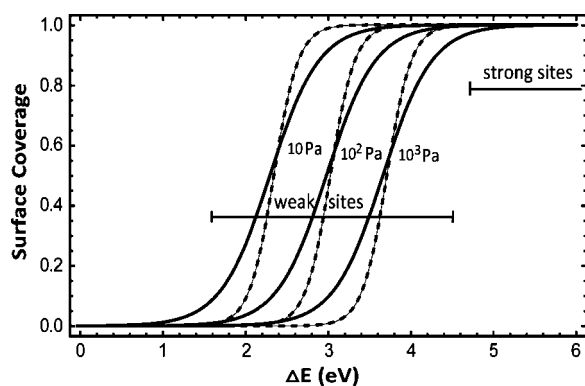
Figure 5. Raman spectrum of pyrolytic carbon.

Figure 6. Calculated surface coverage (θ) vs adsorption enthalpy (ΔE) at 1440 °C and P_{H_2} = 10, 10^2, and 10^3 Pa. The solid lines are for dissociative adsorption; the dashed lines are for molecular adsorption.

function of adsorption enthalpy based on a Langmuir isotherm[34] (Figure 6). This relationship is in accordance with hydrogen–graphite adsorption experiments at high temperatures (600−1800 K) and a wide range of hydrogen pressures (0.66∼10^5 Pa) (refs 20 and 32). The calculation is presented in the Supporting Information.

Three characteristic situations can be identified from Figure 6. When ΔE > 4.5 eV, corresponding to strong adsorption sites at in-plane defects and interstitial loops, the sites are nearly fully occupied regardless of P_{H_2}. In this case, the amount of hydrogen adsorbed on these sites will remain constant even as each analyte peak passes and P_{H_2} fluctuates significantly. However, while there will be no net transfer of hydrogen, D/H exchange between adsorbed and gaseous hydrogen will still proceed at the desorption rate, $t_{1/2}$ estimated via the Arrhenius equation to be >10^0 s. Kinetic isotope effects accompanying this exchange are expected to be negligible at such a high temperature. Equilibrium isotope effects may well exist, but they would affect all peaks equally and thus could not contribute to memory.

Hydrogen adsorbed to strong sites can thus be viewed as a pool of constant size but varying isotopic composition. It is continuously equilibrating with H_2 in the gas phase but on a time

scale similar to that of the chromatographic separation. It will initially be in isotopic equilibrium with background hydrogen, but as an analyte peak passes through the reactor the D/H ratio of the adsorbed hydrogen pool will shift toward that of the analyte. If a second peak arrives before the adsorbed pool has fully re-equilibrated with the background, then a memory effect will be induced. The size of the adsorbed pool, and thus the resulting memory effect, is governed by the amount and structure of carbonaceous material in the pyrolysis reactor.

The second situation arises when 1.5 eV < ΔE < 4.5 eV, corresponding to weak adsorption sites at relaxed edges of the graphite plane. In this case, equilibrium surface coverage varies substantially and rapidly with P_{H_2}. There will be net transfer of hydrogen into the adsorbed pool when an analyte peak is present and P_{H_2} is high, followed by net transfer of hydrogen into the gas phase once that peak passes. The speed of this equilibration (10^{-7} s < $t_{1/2}$ < 10^0 s) precludes it from producing memory effects that can span tens of seconds, but it can result in peak tailing. An analogous situation familiar to chromatographers occurs when analytes are weakly and reversibly adsorbed onto bare silica or metal surfaces. The third situation, in which ΔE < 1.5 eV, includes molecular and dissociative adsorption onto aromatic planes. Hydrogen adsorption on these sites is negligible at 1440 °C, and can be ignored.

In a real pyrolysis reactor, there is a temperature gradient from GC oven temperature at the inlet up to 1440 °C at the middle. Because pyrolytic conversion of organic compounds to H_2 is incomplete at the lower temperatures,[2] as analytes traverse this zone they may deposit partial pyrolysis products on the reactor walls. H atoms on these organic fragments are conceptually equivalent to chemisorbed H. They can undergo exchange with gaseous H_2 according to the same mechanisms but with slower kinetics due to the lower temperatures. This process might also explain the extra memory effect observed when H_2 gas is used instead of CH_4 to generate peak 2 (expt D), if the temperature in this zone is sufficient to promote exchange with H_2 but insufficient to pyrolyze CH_4. Hydrogen exchange in the form of CH_4 molecules seems unlikely because the adsorption heat of CH_4 on graphite is only 0.14 eV (ref 35), resulting in negligible surface coverage at the relevant temperatures.

Model of Memory Effects. As the preceding discussion demonstrates, only strong-site adsorption is capable of producing memory effects spanning tens of seconds. To understand whether the experimentally observed memory effects can be quantitatively described by this phenomenon, we constructed a numerical model that simulates hydrogen isotopic exchange between gas-phase and adsorbed hydrogen. A detailed description of the model algorithm and choice of relevant parameters is provided in the Supporting Information. Model results indicate that memory effects due to changes in δD between pairs of otherwise identical peaks (i.e., expts A and B) can be fully explained by strong-site adsorption (dashed line in Figure 2). Parameters used in the model were tuned to match the data from expt B, and the same values were then used for simulation of subsequent experiments. So while the near-perfect agreement of model and experiment in Figure 2 is the result of model tuning, the prediction of a linear dependence

(34) Billing, G. D. *Dynamics of Molecule Surface Interactions*; John Wiley & Sons Inc.: New York, 2000.

(35) Albesa, A. G.; Llanos, J. L.; Vicente, J. L. *Langmuir* **2008**, *24*, 3836–3840.

of the δD value for peak 2 on the δD value of peak 1 is robust regardless of chosen parameters.

In model simulations of experiments in which Δt varies (Figure 3a,b), the model produces a drop in δD values for peak 2 with increasing Δt as in the experiments, but the change is much faster. The rate of change in the model results is controlled primarily by the choice of desorption rate constant and adsorption pool size, which are derived from published data for pyrolytic carbon.[20] Our model could closely replicate the shape of the experimental data in Figure 3, but doing so requires an unrealistically strong C−H bond dissociation energy (e.g., > ~5 eV), resulting in slow desorption, and a huge number of strong adsorption sites in the pyrolytic carbon (concentration >500 appm). Similarly, model simulations of experiments in which analyte abundance varies (Figure 4a) reproduce the general trend of increasing δD value for peak 2 with an increasing A_2/A_1 ratio but rise more rapidly than the observations. The modeled δD of peak 2 was enriched by 430‰ over a 10-fold increase of analyte abundance, which is much more sensitive than the observation. In this case, the rate of rise in δD value of peak 2 with changing A_2/A_1 ratio depends mainly on the choice of background δD value. A background δD value of +250‰ yields model results that accurately reproduce the slope of experimental data (not shown), but this value is unrealistically high for the true hydrogen background. Possible causes for these discrepancies are discussed below.

DISCUSSION

Model Simulations of Experimental Data. Our model for hydrogen adsorption on graphite reproduces many of the general features of the experimental data, suggesting that this mechanism is an important component of isotopic memory in GC/P/IRMS systems. There are, however, significant differences in detail. This is perhaps not surprising given that many other processes are not accounted for in the model. For example, hydrogen exchange within the GC system, which accounts for up to half of the memory affecting organic analytes, is not considered and the kinetic characteristics of this process are essentially unknown. Moreover, the carbonaceous material lining the pyrolysis reactor is a three-dimensional structure, and so diffusion of H_2 into and out of the carbonaceous material will affect exchange rates. Reported values of the hydrogen diffusion coefficient in carbonaceous materials range from 10^{-12} to 10^{-17} m^2/s at 1440 °C (ref 36). Assuming a thickness for the pyrolytic carbon to be 10 μm, the characteristic diffusion time for H_2 will be minutes to years. This process may explain much of the difference between model and experiment when Δt is varied (e.g., Figure 3), wherein observed memory effects are sustained much longer than predicted by model simulations. Indeed, our model most accurately simulates these experiments using unrealistically slow desorption rates. Additionally, hydrogen exchange near the ends of the pyrolysis reactor that are ≪1440 °C might also result in slower kinetics.

Other potential differences between the model and experiment include the pressure dependence of several hydrogen seclusion mechanisms, such as gas storage within porosity or molecular flow through microfractures in the pyrolysis tube. Because P_{H_2} varies significantly with peak size, these effects may partially explain the differences between the model and observation when A_2/A_1 abundance ratios are varied (Figure

4a). Finally, the model assumes background hydrogen with a fixed abundance and δD value. Background hydrogen likely derives from a combination of column bleed, water in the carrier gas and/or air leaks, and a slow release of absorbed hydrogen from wall materials, all of which are likely to vary over the course of a single GC analysis.

Impact and Mitigation of Memory Effects in Complex Samples. The number of different parameters contributing to isotopic memory in GC/P/IRMS systems makes it impractical to predict, or correct for, memory in all but the simplest of chromatograms. For complex chromatograms with closely spaced peaks, uncertainty contributed by memory effects can be approximately estimated as follows. Assuming an average value for M of 4%, the added uncertainty in the δD value of each peak will be roughly 0.04 times the difference in δD value between that peak and the preceding peak. Differences in peak spacing, height, background size and composition, pyrolysis tube age, and other factors will all affect this estimate but are second-order effects. Given a typical analytical precision for δD values of ~4‰, we suggest that, as a rule of thumb, memory effects will become significant when peaks vary in δD values by more than 100‰. This threshold is frequently exceeded when comparing, for example, n-alkyl and isoprenoid lipids[37] or when measuring D-enriched samples against natural abundance standards.[17,38]

Our results further suggest several ways in which the impact of isotopic memory can be mitigated. First, decreasing the amount of pyrolytic carbon in the reactor, either by replacing the reactor frequently or by heating in an oxidizing atmosphere, should help minimize memory. However, this needs to be balanced against the necessity of "conditioning" new pyrolysis reactors to achieve quantitative pyrolysis.[39] Second, we emphasize the importance of comparing unknown analytes to reference peaks of similar δD value to minimize systematic errors due to memory. This recommendation is currently problematic due to the lack of D-enriched standards. We are therefore making nine of our D-enriched fatty acid ester standards, with δD values ranging from +1.5 to +552‰, available to the community at nominal cost. They may be obtained from Arndt Schimmelmann at Indiana University (http://php.indiana.edu/~aschimme/hc.html). Third, the insertion of peaks of constant δD value into a chromatogram, either by coinjection of standards or via an organic reference gas such as described here, will help to stabilize the isotopic composition of pools of exchangeable hydrogen that lead to memory effects. This procedure does not reduce the amount of memory but does help to ensure a more consistent offset due to memory. In samples where differences in δD between analytes are more important than absolute δD values, this approach will be beneficial. Finally, our model simulations suggest that a higher hydrogen background will serve a similar function, rapidly returning the pool of exchangeable hydrogen to a constant D/H ratio. We have not yet tested this prediction.

A further difficulty is encountered in the common "normalization" procedure used to ensure that δD data from different

(36) Atsumi, H. *Phys. Scr.* **2003**, *T103*, 77–80.

(37) Sessions, A. L.; Burgoyne, T. W.; Schimmelmann, A.; Hayes, J. M. *Org. Geochem.* **1999**, *30*, 1193–1200.

(38) Sessions, A. L.; Jahnke, L. L.; Schimmelmann, A.; Hayes, J. M. *Geochim. Cosmochim. Acta* **2002**, *66*, 3955–3969.

(39) Bilke, S.; Mosandl, A. *Rapid Commun. Mass Spectrom.* **2002**, *16*, 468–472.

laboratories are comparable. For example, the procedure recommended by Sessions et al.[16] is based on measuring a series of 15 *n*-alkanes with δD values ranging from -46‰ to -260‰. However, because these materials were obtained from natural sources, they tend to follow a pattern in which even carbon numbers are D-enriched (near -50‰), and odd carbon numbers are D-depleted (<-120‰). The resulting chromatogram thus has large differences in δD values between most pairs of adjacent peaks. Memory effects will tend to reduce measured differences in δD values between these peaks, leading to the appearance of scale compression. More than 500 analyses of this *n*-alkane standard in our laboratory over the past 4 years reveal a systematic pattern in which the slope and intercept of the normalization line (calculated as the regression of measured δD on "true" δD) systematically decrease from ~ 1 to <0.92 and from ~ 2 to <-10, respectively, as the pyrolysis reactor ages. A simple calculation estimating the impact of memory effects on these analyses indicates that the trend can derive almost entirely from isotopic memory, rather than true scale compression. We therefore recommend that the normalization procedure of Sessions et al.[16] not be employed as described. A simple and robust strategy to separately assess memory effects and scale compression is currently lacking.

CONCLUSIONS

We have conclusively demonstrated the existence of memory effects in compound-specific D/H analyses of organic analytes by GC/P/IRMS. The magnitude of these effects can be quantified as the apparent change in δD value of a given peak relative to the change in δD value of the preceding peak ($\Delta\delta_2/\Delta\delta_1$) and is typically $1-5\%$. In general, memory decreases with increased time separation between peaks and with increased analyte abundance.

Roughly half of this memory appears to originate within the GC system itself, while the other half arises during the pyrolytic conversion of analytes to H_2. Adsorption of hydrogen on carbonaceous material lining the pyrolysis reactor is likely an important mechanism in this latter source of memory. A model for hydrogen adsorption on graphite sites can reproduce many, though not all, of our experimental data using experimentally relevant parameters. As a rule of thumb, these memory effects become significant when adjacent peaks differ in δD value by >100‰. The results emphasize the need to match analytes with reference standards of similar δD value to minimize systematic biases due to isotopic memory effects.

SUPPORTING INFORMATION AVAILABLE

Model description, plots of simulated signal, and mathematical derivation of partitioning algorithms. This material is available free of charge via the Internet at http://pubs.acs.org.